UC Berkeley
UC Berkeley Previously Published Works

Title

Surface Chemically Switchable Ultraviolet Luminescence from Interfacial Two-Dimensional Electron Gas

Permalink

https://escholarship.org/uc/item/8ps2599f

Journal

Nano Letters, 16(1)

ISSN

1530-6984

Authors

Islam, Mohammad A
Saldana-Greco, Diomedes
Gu, Zongquan
et al.

Publication Date

2016-01-13

DOI

10.1021/acs.nanolett.5b04461

Peer reviewed

Surface Chemically Switchable Ultraviolet Luminescence from Interfacial Two-Dimensional Electron Gas

Mohammad A. Islam,[†] Diomedes Saldana-Greco,[‡] Zongquan Gu,[§] Fenggong Wang,[‡] Eric Breckenfeld,[∥] Qingyu Lei,[⊥] Ruijuan Xu,[#] Christopher J. Hawley,[†] X. X. Xi,[⊥] Lane W. Martin,[#] Andrew M. Rappe,[‡] and Jonathan E. Spanier*,[†,§,∇]

[†]Department of Materials Science & Engineering, [§]Department of Electrical & Computer Engineering, and [∇]Department of Physics, Drexel University, Philadelphia, Pennsylvania 19104, United States

[‡]The Makineni Theoretical Laboratories, Department of Chemistry, University of Pennsylvania, Philadelphia, Pennsylvania 19104, United States

[∥]Department of Materials Science & Engineering, University of Illinois at Urbana–Champaign, Urbana, Illinois 61801, United States

[⊥]Department of Physics, Temple University, Philadelphia, Pennsylvania 19122, United States

[#]Department of Materials Science and Engineering, University of California, Berkeley, Berkeley, California 94720, United States

S *Supporting Information*
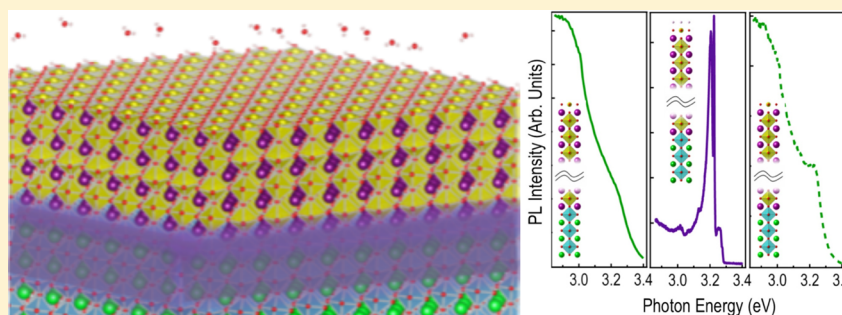
ABSTRACT: We report intense, narrow line-width, surface chemisorption-activated and reversible ultraviolet (UV) photoluminescence from radiative recombination of the two-dimensional electron gas (2DEG) with photoexcited holes at $LaAlO_3/SrTiO_3$. The switchable luminescence arises from an electron transfer-driven modification of the electronic structure via H-chemisorption onto the AlO_2-terminated surface of $LaAlO_3$, at least 2 nm away from the interface. The control of the onset of emission and its intensity are functionalities that go beyond the luminescence of compound semiconductor quantum wells. Connections between reversible chemisorption, fast electron transfer, and quantum-well luminescence suggest a new model for surface chemically reconfigurable solid-state UV optoelectronics and molecular sensing.

KEYWORDS: *Two-dimensional electron gas, photoluminescence, $LaAlO_3/SrTiO_3$, chemisorption*

The well-known *polar catastrophe* model[1,2] explains the $LaAlO_3$-thickness-dependent insulator-to-metal transition in $LaAlO_3/SrTiO_3$, with its electronic reconstruction consisting of holes at the surface and electrons at the interface, due to potential buildup across $LaAlO_3$. The resulting conducting interfacial state is distinctly different from the 2DEG at a conventional semiconductor heterojunction located at an interface deep below the surface[3] or at a semiconductor surface due to metal atom adsorption[4,5] or intrinsic electron accumulation.[6−8] The electronic structure and correlations in $LaAlO_3/SrTiO_3$ drive a host of unique features and findings in this interfacial 2DEG, including magnetic[9] and superconducting ordering[10] and room-temperature local surface-controlled switching of conductance[11] and of photoconductivity.[12] The interfacial conductance and functionality depend on the free surface. Capping the $LaAlO_3$ surface with metallic contacts,[13]

metal oxides,[14] or polar solvents[15] accommodates the electrostatics of the system, stabilizing the electronic reconstruction and increasing the electron density at the interface. This increment of the 2D electron density via surface modulation could advance light-emission technology involving these interfacial states. However, direct access to these conducting states is a remarkable challenge, since overlapping conduction and valence bands, internal electric fields within $LaAlO_3$, low 2D electron density in bare $LaAlO_3/SrTiO_3$, and radiative recombination through O vacancies each contribute to preventing the observation of sharp optical transitions involving the interfacial states. The few photoluminescence (PL) studies on this system have mainly focused on the oxygen-deficient
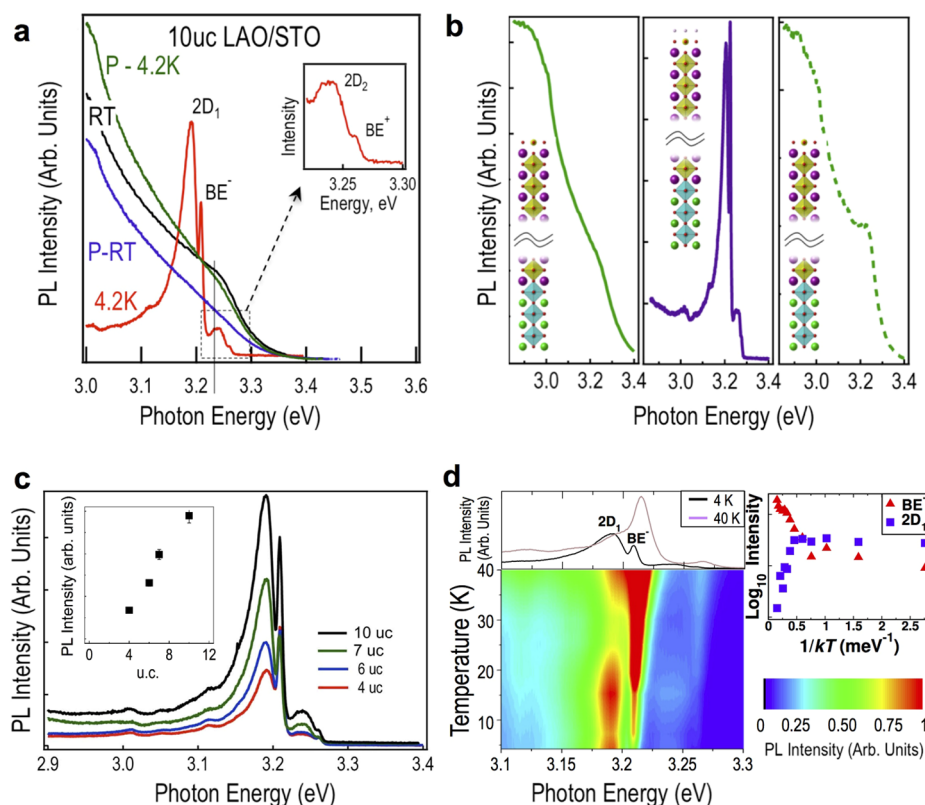
Figure 1. Absorption-induced optical transitions in complex oxide quantum well. (a) PL from a pristine (P) ten-unit-cell film of $LaAlO_3$ on $SrTiO_3$ bulk shows a broad feature (≈ 2.8 eV) attributed to recombination involving O vacancies. When the sample is exposed to water vapor in situ under vacuum, 300 K PL remains broad (black trace). Significantly, intense UV PL peaks emerge at 4.2 K (red trace). Peaks denoted $2D_1$ and $2D_2$ (inset) are assigned to different 2D quantized electronic energy level recombination with free holes. Peaks denoted zone boundary edge (BE^- and BE^+, inset) are assigned to phonon-assisted interband transitions in $SrTiO_3$. (b) Reversibility of PL spectrum from a single $LaAlO_3/SrTiO_3$ film heterostructure as found (left), following H-chemisorption (center), and after annealing in O_2 and desorption of H (right), each collected at 4.2 K. (c) PL intensity collected at 4.2 K in $LaAlO_3/SrTiO_3$ samples exposed to water vapor in the same manner as described in the main text, with 4, 6, 7, and 10 unit cells (u. c.) of $LaAlO_3$, revealing a thickness dependence to the PL intensity. Shown in the inset are the integrated PL intensities for the $2D_1$ peak at different unit cells thickness of $LaAlO_3$. (d) Temperature evolution of the PL from $LaAlO_3/SrTiO_3$ with the PL intensity legend on the side. Shown in the upper inset are the PL spectra at 4 and 40 K indicating the $2D_1$ and BE^- peaks. In the side inset are the integrated intensities of the 2DEG and BE^- peaks plotted as functions of $1/kT$. Unlike the phonon-assisted PL peak, which decreases with decreasing T, cooling-induced onset and rise of the 2DEG peak is observed, followed by its saturation at lower T. This is a signature of the onset of spatial confinement of carriers, as found in classic III–V and III–N semiconductor heterojunction 2DEGs.

$SrTiO_3$ within the heterostructure,[16] except for a recent report indicating broad PL signatures thought to arise from two-carrier radiative recombination of the interface induced electrons and photoexcited holes.[17]

In this Letter we demonstrate, through a combination of PL spectroscopy, density functional theory (DFT) simulations, Poisson-Schrödinger modeling, and thermodynamic analysis, a novel manifestation of PL properties from quantum well structures in oxide materials. We show that chemisorption-induced manipulation of the interfacial electronic structure can reversibly induce and suppress intense ultraviolet (UV) PL involving radiative recombination of electrons confined at the $LaAlO_3/SrTiO_3$ interface with photoinduced holes. Our studies reveal that the dissociated water fragments on the surface unentangle the interfacial electron density, allowing for direct optical examination of these states. DFT calculations elucidate the atomistic and electronic mechanism by which the H-chemisorption onto $LaAlO_3/SrTiO_3$ enables the system to reach potential and charge equilibrium. Chemisorption eliminates the average electric field in $LaAlO_3$ and increases the 2D carrier density in the quantized states at the interface, providing strong, accessible transitions in the near UV.

The PL measurements were performed on one set of 10 unit cells thick $LaAlO_3$ films, which were grown via reflection high-energy electron diffraction (RHEED)-monitored pulsed-laser deposition (PLD). The films were grown at a substrate temperature of 750 °C (this is the temperature of the Ag-paint used to provide thermal contact between the substrate and the heater plate, as measured via pyrometry), in an oxygen pressure of 1×10^{-3} Torr, with a laser repetition rate of 1 Hz, from a single crystal $LaAlO_3$ (001) target (Crystec, GmbH) on TiO_2-terminated $SrTiO_3$(001) substrates treated via standard methods. PL spectra were collected through a 0.3 m monochromator (Jobin Yvon U1000, Edison NJ), dispersed with 1200 grooves/mm gratings, and detected using a water-cooled photomultiplier tube (Hamamatsu). A 325 nm He–Cd laser (Kimmon-Khoa) was used as the excitation source, focused to a spot diameter of 1.15 μm. The incident intensity was in the range of 1–22 W/cm². The samples were mounted in a cryostat (Janis ST-100) and held at 5×10^{-6} Torr (see Supporting Information).

The atomic and electronic structures of this system were computed via plane-wave basis set DFT using the local density approximation[18] + Hubbard U method (LDA + U)[19] as
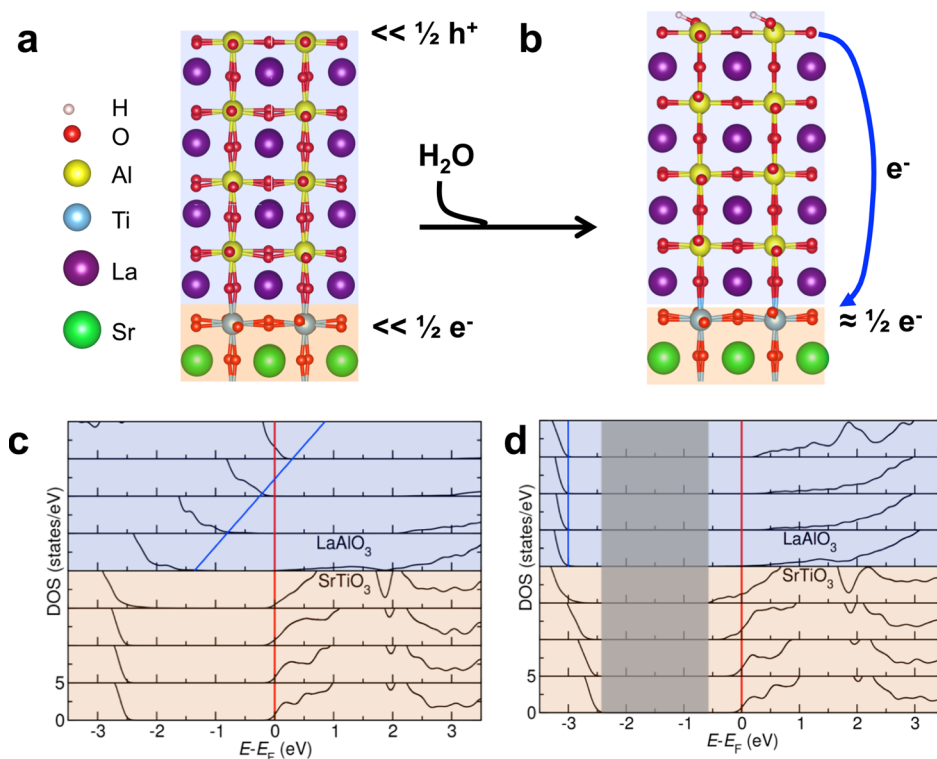
Figure 2. Access to optical transitions from the 2DEG. The atomic structure of the oxide heterostructure quantum well interface of (a) bare $LaAlO_3$/$SrTiO_3$, indicating that the hole density at the surface and the electron density at the interface are far smaller than the $1/2$ hole/electron per surface unit cell at the infinite thickness limit, and (b) H-chemisorbed $LaAlO_3$/$SrTiO_3$ resulting in higher density of localized 2D confined electrons at the interface. Once the H atoms are chemisorbed on the surface, the holes are passivated, driving complete electron transfer to the interface, illustrated by the solid blue arrow. (c) Layer-resolved electronic density of states (DOS) for bare $LaAlO_3$/$SrTiO_3$ undergoing the polar catastrophe, with the blue line indicating the potential buildup. The potential buildup provides states that will inhibit sharp optical transitions. (d) Layer-resolved DOS after chemisorption of H onto $LaAlO_3$/$SrTiO_3$. The H atom transfers an electron to the $LaAlO_3$/$SrTiO_3$ interface at equilibrium, eliminating the potential build up and opening an energy gap, so that optical transitions can be accessed, indicated by the gray shaded area.

implemented in the Quantum Espresso[20] computer code. All atoms were represented by norm-conserving, optimized,[21] designed nonlocal[22] pseudopotentials generated with the Opium package[23] (see Supplementary).

To probe the optical properties of the interfacial electronic structure, a series of temperature-dependent PL measurements were performed under two distinct sample treatments. The PL spectra collected at both 4.2 K and room temperature (RT) from as-grown ten-unit-cell films of $LaAlO_3$ on $SrTiO_3$ bulk samples (Supplementary Figure S1) stored at 300 K and atmospheric pressure (denoted as "pristine") reveal a peak near 2.8 eV with a broad PL feature (see Figure 1a). This signal is attributed to radiative recombination through oxygen vacancy defect levels.[16] When the sample is briefly (1 s) exposed to water vapor in situ under vacuum at room temperature, the PL spectra collected still have the broad character.

However, the PL spectra at 4.2 K from identical samples collected immediately following 1 s exposure to water vapor, while under vacuum possess sharp UV features and nearly complete suppression of the broad lower-energy emission (Figure 1a). Peaks at 3.209 and 3.261 eV (BE^- and BE^+, respectively) are assigned to interband transitions involving transverse optical phonon ($\omega_{TO} = 26$ meV) emission ($E_g - \hbar\omega_{TO}$) and absorption ($E_g + \hbar\omega_{TO}$) at the Brillouin zone boundary edge.[24] Phonon-assisted PL is commonly seen in indirect band gap materials like $SrTiO_3$, and the absence of excitons is consistent with its unusually high dielectric constant ($\approx 10,000$ at 4.2 K).[25] We thus estimate E_g of our $SrTiO_3$

samples to be 3.235 eV at 4.2 K, in agreement with previous reports.[26]

We propose that the strong, sharp peak centered at 3.192 eV and the smaller peak at 3.240 eV ($2D_1$ and $2D_2$, respectively, Figure 1a), originate from radiative recombination of two-dimensionally confined electrons at the $LaAlO_3$/$SrTiO_3$ interface with photoexcited holes. The strong $2D_1$ and well-defined $2D_2$ PL signals directly relate to the surface chemical state. After water exposure, the original broad 2.8 eV-centered PL can be recovered through ex situ O_2 annealing; subsequent exposure to water in situ again produces the identical strong $2D_1$ and well-defined $2D_2$, higher-energy PL features and suppresses the broad lower energy emission. This off-on-off process, driven by ex situ O_2 annealing, exposure to water, and further O_2 annealing, operates reproducibly in each sample tested (see Figure 1b). This strongly suggests that the PL associated with the 2DEG quantum wells is tuned by the strong coupling between the surface and interfacial electronic states.

There have been reports of changes in the electronic structure in conventional semiconductor heterostructure 2DEGs due to gating from distant surface adsorbates.[3] In addition, irreversible changes in 2DEG electronic structure at surfaces due to metal[4] or molecular[27−30] adsorption have also been observed. Here we show, experimentally and theoretically, reversible changes in PL from the interface due to electrostatically accessible, but chemically inaccessible 2DEG. Tunability of the sharp 2DEG-photoexcited hole PL in our water-treated $LaAlO_3$/$SrTiO_3$ samples is achieved even at distances of ≈ 2 nm
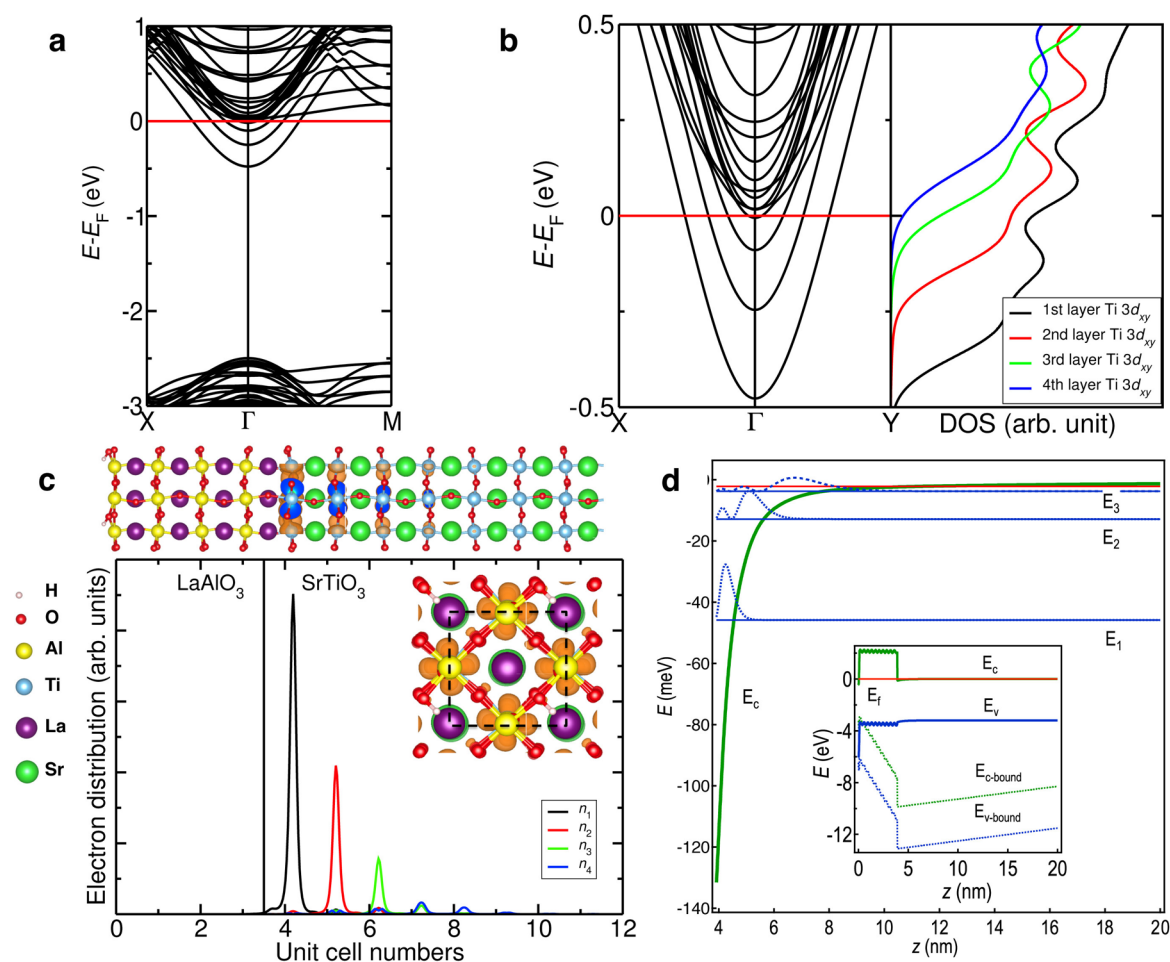
Figure 3. Influence of H$^+$ on electronic structure. (a) DFT calculated electronic band structure of H$^+$ surface-chemisorbed LaAlO$_3$/SrTiO$_3$ showing a large valence-conduction band gap. (b) Left panel: enlarged view of the conduction states in a; right panel: the projected DOS shows the contribution from the Ti 3d$_{xy}$ orbitals in the layers near the interface. The red line indicates E_F. (c) Electron distribution of the conduction states. The atomic structure at the top of the graph shows a charge density isosurface for all the states within 0.5 eV below E_F, which consists of $n = 4$ bands. The graph below shows the planar-averaged filled state density of the conduction bands. The inset shows that the conduction electrons are strongly localized in Ti 3d$_{xy}$ orbitals. (d) Self-consistent Poisson-Schrödinger model calculations show (inset) that passivation of AlO$_2$-terminated LaAlO$_3$/SrTiO$_3$ by H$^+$ results in flattening of the conduction (solid green) and valence (solid blue) bands in LaAlO$_3$ ($0 < z < 4$ nm) compared with the bound potential (dashed green and blue, respectively) induced by AlO$_2$ and LaO, consistent with the DFT results in Figure 2c and d. Band bending (green), bound eigenstates (horizontal blue), and the modulus of the electronic eigenfunctions (blue) are shown and contribute to observed 2DEG-photoexcited hole PL.

between the free surface and the 2DEG interfacial quantum well. Figure 1c shows the quantum well PL signatures of the spectra collected at 4.2 K in LaAlO$_3$/SrTiO$_3$ samples with 4, 6, 7, and 10 unit cells of LaAlO$_3$ grown under the same conditions and exposed to water vapor. The fitted PL intensity increases for larger numbers of LaAlO$_3$ unit cells, along with the evolution of interfacial electronic reconstruction as a function of LaAlO$_3$ film thickness (see Supporting Information).

A distinctive signature of the two-dimensional origin of the PL is saturation of the 2DEG PL intensity at low T followed by thermally activated quenching at higher T.[31,32] The LaAlO$_3$/SrTiO$_3$ 2DEG PL can be discerned in our spectra beginning at $\approx$40 K (Figure 1d). Its intensity rises for decreasing T with an activation energy of 8.06 meV, saturating at $\approx$23 K, which it is roughly constant (Figure 1d, inset). This activation and saturation signify thermally induced leakage of a critical density of carriers out of the interfacial quantum well into the bulk, and a 2D electron-photoexcited hole radiative recombination rate that exceeds the rate of carrier leakage, respectively. In stark

contrast, the intensities of the phonon-mediated PL peaks (BE$^-$, BE$^+$) exhibit a steady rise with T and are well-discerned even for $T > 200$ K.

The optical transitions from the 2DEG quantum well are controlled by the adsorbate dynamics on the AlO$_2$ surface layer. The H$_2$O molecules spontaneously dissociate into H$^+$ and $^-$OH when the AlO$_2$-terminated LaAlO$_3$/SrTiO$_3$ system is exposed to water vapor, enabling the "water-cycle" mechanism.[33] The dissociated H$_2$O components can diffuse and influence the surface environment. Specifically, the dissociated $^-$OH can fill a surface O vacancy and become an adsorbed H$^+$, reducing the number of O vacancies. However, dissociated H$^+$ has lower diffusion barriers than $^-$OH,[34] leading to large surface regions populated mainly by H$^+$. Our ab initio thermodynamic stability analysis of surfaces covered with either $^-$OH or H$^+$ shows that the H-chemisorbed system is much more stable than the OH-chemisorbed system (Supplementary Figure S2). The relaxed atomic structures of the bare and H-chemisorbed LaAlO$_3$/SrTiO$_3$ systems are shown in Figure 2a and b, respectively.

Previous work on H-chemisorbed-LaAlO$_3$/SrTiO$_3$ indicates that the most stable coverage is one H per two surface unit cells,[35] and our DFT+U[19] calculations show that this coverage leads to full elimination of the potential buildup which originally resides on the bare surface (Figure 2c and d). The calculated electronic structures for the four-layer LaAlO$_3$/eight-layer SrTiO$_3$ (001) system with chemisorbed H$_2$O and OH show typical metallic features, similar to bare LaAlO$_3$/SrTiO$_3$ (Supplementary Figure S3 and S4); however, the H-chemisorbed system is strikingly different. The electronic structure of the H-chemisorbed LaAlO$_3$/SrTiO$_3$ system differs from that of the bare system due to complete passivation of the surface charge. This translates into higher 2D electron density of 3.71×10^{14} electrons cm^{-2} for the H-chemisorbed LaAlO$_3$/SrTiO$_3$ system, while the bare system shows 2.31×10^{13} electrons cm^{-2} (Figure 2c and d). This occurs via electron transfer from the surface chemisorbed H to the interface, removing the "polar catastrophe". Cancellation of the potential build up in LaAlO$_3$ unentangles the overlap between the conduction and valence bands, opening a gap in the spectrum (Figure 3a). This yields an isolated 2DEG, which consists of populating the Ti 3d states in the first few SrTiO$_3$ unit cells near the interface (Figures 3b, 3c). These states give a higher 2DEG density, enabling strong optical transitions at the interface and suppressing signals from deeper in the material, as observed experimentally. Though underestimated by DFT+U, the calculated $E_g \approx 2.1$ eV (Figure 3a, Supplementary Figure S5), taken together with the resulting high electron density, indicate that sharp radiative band-to-band transitions are due to H chemisorption.

The UV PL features arise from radiative recombination of electrons in quantized states with photoexcited holes. Our DFT calculations predict strongly localized 2DEG conducting states below E_F. These states mainly arise from Ti 3d$_{xy}$ orbitals at and near the interface (Figure 3b). The spatially resolved electron distribution of these conducting states clearly shows that the 2DEG is distributed into four SrTiO$_3$ unit cells, strongly localized at the TiO$_2$ layers, with lower density farther from the LaAlO$_3$ interface (Figure 3c). These features indicate that the confining potential from the interfacial band bending has significant contributions from multiple quantum wells each spaced by an oxygen octahedral distance.

To further analyze the 2DEG-derived PL features, we consider how chemisorption of H$^+$ on AlO$_2$ surfaces of LaAlO$_3$ alters the conduction and valence bands at and near the LaAlO$_3$/SrTiO$_3$ interface and induces changes in electron density, band bending, and formation of quantized 2D sub-bands at and near the interface. Self-consistent solutions of the coupled Poisson-Schrödinger eqs (Supporting Information) including band-bending[36] reveal H$^+$ chemisorption-induced flattening of the potential gradient across the LaAlO$_3$ layer, and that the calculated $n = 1$ level is 42 meV below the bulk band edge (Figure 3d, Supplementary Figure S6), in excellent agreement with our measured value of 43 meV.

The removal of the electrostatic slope in the LaAlO$_3$ overlayer causes all of the transitions to have the same energy. In the absence of the H$^+$ adsorption, radiative recombination of a photoexcited hole in the surface layer would result in a different photon energy than that for a hole in a subsurface LaAlO$_3$ layer. Following H$^+$ adsorption, all LaAlO$_3$ layers provide equi-energetic holes. As the LaAlO$_3$ overlayer is made thicker, it gradually passivates the polar catastrophe, only completely doing so in the thick film limit. Here, by providing a higher-energy source of electrons (thereby stabilizing surface holes) H allows the few layers of LaAlO$_3$-topped hetero-structure to 100% passivate the polar catastrophe, making the potential flat and the PL sharp. This leads to our observation of a much more dramatic change in PL than one would see by thickening the LaAlO$_3$ incrementally.

This system provides a convenient external control of 2DEG properties that offers reversible switching between sharp UV and broad blue photoluminescence. This is fundamentally interesting physics, and this significant change in PL could be harnessed as a signal in a photonic circuit or relay, or as a sensitive new in operando probe of surface molecular adsorption since these results are observed in a non-UHV environment and water dissociated species are proxies for other electron-donating adsorbate species.[15] Realization of these concepts in the UV and their strong dependence on the environment opens up new opportunities and challenges. Such a system could provide new optoelectronic devices that operate at short wavelengths.

■ ASSOCIATED CONTENT

ⓢ Supporting Information

The Supporting Information is available free of charge on the ACS Publications website at DOI: 10.1021/acs.nano-lett.5b04461.

> Film growth, photoluminescence of LaAlO$_3$/SrTiO$_3$ films; thermodynamic stability analysis of H$^+$ and $^-$OH adsorption on the LaAlO$_3$/SrTiO$_3$ surface; density functional theory calculations of LaAlO$_3$/SrTiO$_3$; and self-consistent Poisson-Schrödinger model (PDF)

■ AUTHOR INFORMATION

Corresponding Author

*Phone: +1 215.895.2301. E-mail: spanier@drexel.edu.

Author Contributions

M.A.I. and D.S.-G. contributed equally to this work.

Notes

The authors declare no competing financial interest.

■ REFERENCES

(1) Ohtomo, A.; Hwang, H. Y. Magnetization and Energy Gaps of a High-Mobility 2D Electron Gas in the Quantum Limit. *Nature* **2004**, *427*, 423−426.

(2) Breitschaft, M.; Tinkl, V.; Pavlenko, N.; Paetel, S.; Richter, C.; Kirtley, J. R.; Liao, Y. C.; Hammerl, G.; Eyert, V.; Kopp, T.; Mannhart, J. Two-dimensional electron liquid state at $LaAlO_3$-$SrTiO_3$ interfaces. *Phys. Rev. B: Condens. Matter Mater. Phys.* **2010**, *81*, 153414.

(3) Neuberger, R.; Müller, G.; Ambacher, O.; Stutzmann, M. High-Electron-Mobility AlGaN/GaN Transistors (HEMTs) for Fluid Monitoring Applications. *physica status solidi (a)* **2001**, *185*, 85−89.

(4) Biagi, R.; Corradini, V.; Bertoni, G.; Mariani, C.; del Pennino, U.; Grazia Betti, M. Single-particle and collective excitations of a two-dimensional electron gas at the Cs/InAs(110) surface. *Phys. Rev. B: Condens. Matter Mater. Phys.* **2001**, *64*, 195407.

(5) Rickert, K. A.; Ellis, A. B.; Himpsel, F. J.; Lu, H.; Schaff, W.; Redwing, J. M.; Dwikusuma, F.; Kuech, T. F. X-ray photoemission spectroscopic investigation of surface treatments, metal deposition, and electron accumulation on InN. *Appl. Phys. Lett.* **2003**, *82*, 3254.

(6) Veal, T. D.; Mahboob, I.; Piper, L. F. J.; McConville, C. F.; Lu, H.; Schaff, W. J. Indium nitride: Evidence of electron accumulation. *J. Vac. Sci. Technol., B: Microelectron. Process. Phenom.* **2004**, *22*, 2175.

(7) Mahboob, I.; Veal, T. D.; Piper, L. F. J.; McConville, C. F.; Lu, H.; Schaff, W. J.; Furthmüller, J.; Bechstedt, F. Origin of electron accumulation at wurtzite InN surfaces. *Phys. Rev. B: Condens. Matter Mater. Phys.* **2004**, *69*, 201307.

(8) Mahboob, I.; Veal, T. D.; McConville, C. F.; Lu, H.; Schaff, W. J. Intrinsic Electron Accumulation at Clean InN Surfaces. *Phys. Rev. Lett.* **2004**, *92*, 036804.

(9) Brinkman, A.; Huijben, M.; van Zalk, M.; Huijben, J.; Zeitler, U.; Maan, J. C.; van der Wiel, W. G.; Rijnders, G.; Blank, D. H. A.; Hilgenkamp, H. Magnetic effects at the interface between non-magnetic oxides. *Nat. Mater.* **2007**, *6*, 493−496.

(10) Reyren, N.; Thiel, S.; Caviglia, A. D.; Kourkoutis, L. F.; Hammerl, G.; Richter, C.; Schneider, C. W.; Kopp, T.; Rüetschi, A.-S.; Jaccard, D.; Gabay, M.; Muller, D. A.; Triscone, J.-M.; Mannhart, J. Superconducting Interfaces Between Insulating Oxides. *Science* **2007**, *317*, 1196−1199.

(11) Bark, C. W.; Sharma, P.; Wang, Y.; Baek, S. H.; Lee, S.; Ryu, S.; Folkman, C. M.; Paudel, T. R.; Kumar, A.; Kalinin, S. V.; Sokolov, A.; Tsymbal, E. Y.; Rzchowski, M. S.; Gruverman, A.; Eom, C. B. Switchable Induced Polarization in $SrTiO_3$/$LaAlO_3$ Heterostructures. *Nano Lett.* **2012**, *12*, 1765−1771.

(12) Tebano, A.; Fabbri, E.; Pergolesi, D.; Balestrino, G.; Traversa, E. Room-Temperature Giant Persistent Photoconductivity in $SrTiO_3$/$LaAlO_3$ Heterostructures. *ACS Nano* **2012**, *6*, 1278−1283.

(13) Arras, R.; Ruiz, V. G.; Pickett, W. E.; Pentcheva, R. Tuning the two-dimensional electron gas at the $LaAlO3$/$SrTiO_3$(001) interface by metallic contacts. *Phys. Rev. B: Condens. Matter Mater. Phys.* **2012**, *85*, 125404.

(14) Huijben, M.; et al. Defect Engineering in Oxide Heterostructures by Enhanced Oxygen Surface Exchange. *Adv. Funct. Mater.* **2013**, *23*, 5240−5248.

(15) Xie, Y.; Hikita, Y.; Bell, C.; Hwang, H. Y. Control of electronic conduction at an oxide heterointerface using surface polar adsorbates. *Nat. Commun.* **2011**, *2*, 494.

(16) Kalabukhov, A.; Gunnarsson, R.; Börjesson, J.; Olsson, E.; Claeson, T.; Winkler, D. Effect of oxygen vacancies in the $SrTiO_3$ substrate on the electrical properties of the $LaAlO_3$/$SrTiO_3$ interface. *Phys. Rev. B: Condens. Matter Mater. Phys.* **2007**, *75*, 121404.

(17) Yamada, Y.; Sato, H. K.; Hikita, Y.; Hwang, H. Y.; Kanemitsu, Y. Spatial density profile of electrons near the $LaAlO_3$/$SrTiO_3$ heterointerface revealed by time-resolved photoluminescence spectroscopy. *Appl. Phys. Lett.* **2014**, *104*, 151907.

(18) Perdew, J. P.; Wang, Y. Accurate and simple analytic representation of the electron-gas correlation energy. *Phys. Rev. B: Condens. Matter Mater. Phys.* **1992**, *45*, 13244−13249.

(19) Anisimov, V. I.; Aryasetiawan, F.; Lichtenstein, A. I. First-principles calculations of the electronic structure and spectra of strongly correlated systems: the LDA + U method. *J. Phys.: Condens. Matter* **1997**, *9*, 767.

(20) Giannozzi, P.; et al. QUANTUM ESPRESSO: a modular and open-source software project for quantum simulations of materials. *J. Phys.: Condens. Matter* **2009**, *21*, 395502.

(21) Rappe, A. M.; Rabe, K. M.; Kaxiras, E.; Joannopoulos, J. D. Optimized pseudopotentials. *Phys. Rev. B: Condens. Matter Mater. Phys.* **1990**, *41*, 1227−1230.

(22) Ramer, N. J.; Rappe, A. M. Designed nonlocal pseudopotentials for enhanced transferability. *Phys. Rev. B: Condens. Matter Mater. Phys.* **1999**, *59*, 12471−12478.

(23) http://opium.sourceforge.net (accessed Nov 25, 2015).

(24) Yamada, Y.; Kanemitsu, Y. Band-to-band photoluminescence in $SrTiO_3$. *Phys. Rev. B: Condens. Matter Mater. Phys.* **2010**, *82*, 121103.

(25) Neville, R. C.; Hoeneisen, B.; Mead, C. A. Permittivity of Strontium Titanate. *J. Appl. Phys.* **1972**, *43*, 2124−2131.

(26) Longo, V. M.; de Figueiredo, A. T.; de Lázaro, S.; Gurgel, M. F.; Costa, M. G. S.; Paiva-Santos, C. O.; Varela, J. A.; Longo, E.; Mastelaro, V. R.; De Vicente, F. S.; Hernandes, A. C.; Franco, R. W. A. Structural conditions that leads to photoluminescence emission in $SrTiO_3$: An experimental and theoretical approach. *J. Appl. Phys.* **2008**, *104*, 023515.

(27) Chang, Y.-H.; Lu, Y.-S.; Hong, Y.-L.; Kuo, C.-T.; Gwo, S.; Yeh, J. A. Effects of $(NH_4)_2S_x$ treatment on indium nitride surfaces. *J. Appl. Phys.* **2010**, *107*, 043710.

(28) Eisenhardt, A.; Krischok, S.; Himmerlich, M. Hydrogen adsorbed at N-polar InN: Significant changes in the surface electronic properties. *Phys. Rev. B: Condens. Matter Mater. Phys.* **2015**, *91*, 245305.

(29) Ohashi, N.; Ishigaki, T.; Okada, N.; Taguchi, H.; Sakaguchi, I.; Hishita, S.; Sekiguchi, T.; Haneda, H. Passivation of active recombination centers in ZnO by hydrogen doping. *J. Appl. Phys.* **2003**, *93*, 6386−6392.

(30) Cimalla, V.; Lebedev, V.; Wang, C. Y.; Ali, M.; Ecke, G.; Polyakov, V. M.; Schwierz, F.; Ambacher, O.; Lu, H.; Schaff, W. J. Reduced surface electron accumulation at InN films by ozone induced oxidation. *Appl. Phys. Lett.* **2007**, *90*, 152106.

(31) Bergman, J. P.; Lundström, T.; Monemar, B.; Amano, H.; Akasaki, I. Photoluminescence related to the two-dimensional electron gas at a GaN/AlGaN heterointerface. *Appl. Phys. Lett.* **1996**, *69*, 3456−3458.

(32) Shen, B.; Someya, T.; Moriwaki, O.; Arakawa, Y. Effect of carrier confinement on photoluminescence from modulation-doped $Al_xGa_{1−x}N$/GaN heterostructures. *Appl. Phys. Lett.* **2000**, *76*, 679−681.

(33) Bi, F.; Bogorin, D. F.; Cen, C.; Bark, C. W.; Park, J.-W.; Eom, C.-B.; Levy, J. Water-cycle" mechanism for writing and erasing nanostructures at the $LaAlO_3$/$SrTiO_3$ interface. *Appl. Phys. Lett.* **2010**, *97*, 173110.

(34) Li, F.; Liang, M.; Du, W.; Wang, M.; Feng, Y.; Hu, Z.; Zhang, L.; Wang, E. G. Writing charge into the n-type $LaAlO3$/$SrTiO_3$ interface: A theoretical study of the H_2O kinetics on the top AlO_2 surface. *Appl. Phys. Lett.* **2012**, *101*, 251605.

(35) Son, W.; Cho, E.; Lee, J.; Han, S. Hydrogen adsorption and carrier generation in LaAlO$_3$/SrTiO$_3$ heterointerfaces: a first-principles study. *J. Phys.: Condens. Matter* **2010**, *22*, 315501.

(36) King, P. D. C.; Veal, T. D.; McConville, C. F. Nonparabolic coupled Poisson-Schrödinger solutions for quantized electron accumulation layers: Band bending, charge profile, and subbands at InN surfaces. *Phys. Rev. B: Condens. Matter Mater. Phys.* **2008**, *77*, 125305.